Sensors and Actuators B 262 (2018) 171–179

Contents lists available at ScienceDirect

Sensors and Actuators B: Chemical

journal homepage: www.elsevier.com/locate/snb

Radiometric analysis of UV to near infrared LEDs for optical sensing and radiometric measurements in photochemical systems

Ansara Noori [a], Parvez Mahbub [a], Miloš Dvořák [a,b,c], Arko Lucieer [d], Mirek Macka [a,*]

[a] Australian Centre for Research on Separation Science (ACROSS), School of Physical Sciences University of Tasmania, Private Bag 75, Hobart 7001, Australia
[b] Materials Research Centre, Faculty of Chemistry, Brno University of Technology, Purkyňova 118, 612 00, Brno, Czech Republic
[c] Institute of Analytical Chemistry of the Czech Academy of Sciences, Veveří 967/97, 602 00 Brno, Czech Republic
[d] Discipline of Geography and Spatial Sciences, University of Tasmania, Private Bag 76, Hobart 7001, Australia

ARTICLE INFO

Article history:
Received 28 June 2017
Received in revised form 17 January 2018
Accepted 23 January 2018
Available online 3 February 2018

Keywords:
Light emitting diodes (LEDs)
Optical sensing
Radiometric power output
Irradiance and radiant efficiency
Chemical actinometry
Quantum yield and fluence

ABSTRACT

LEDs have been established as light sources in countless areas of optical sensing and chemical analysis, where they offer a better alternative to traditional light sources in terms of low-cost, small size and robustness supporting portability, and performance parameters such as low noise. However, the lack of rapid, facile and accurate radiometric analysis of LEDs is a major limiting factor which constrains their purposeful use. Therefore, here we present comprehensive radiometric analysis of LEDs in terms of absolute emission spectra, radiometric power output, irradiances, radiant efficiencies as well as uncertainties. This allowed us to develop and cross-validate a rapid, facile, accurate and low-cost radiometric analysis of LEDs with directional light output using a large active area silicon photodiode in a simple optical design with the LED light source in proximity, without the need for a calibrated light source. We demonstrate that data for a wide range of 21 commercial LEDs in UV, vis and NIR spectral range (255–950 nm) agree very well with two entirely independent approaches. First, we obtained an excellent agreement with accuracy within 5% for radiometric power output measured using chemical actinometric methods. Further, we obtained irradiance (mW/cm^2) and radiant efficiency values (%) for the LEDs. The accuracy of irradiance measurement was within 2% when compared with a spectrophotometric method based on a radiometrically calibrated spectrophotometer. The measurement uncertainty at 95% confidence level for values of radiometric power output were reduced 3-fold compared to the existing techniques. We also demonstrate that this facile, accurate and low-cost radiometric analysis can be further extended to accurately measure quantum yield of photochemical reactions and fluence values in actinometric systems.

1. Introduction

Solid state light sources (SSLSs) and specifically light emitting diodes (LEDs) are widely used in analytical chemistry due to their principal advantages including small size, robustness, low cost, long lifetime, quasi-monochromatic emission, and low noise [1,2]. The analytical areas of strong LED usages are wide ranging including optical sensing [1,2], spectrophotometric analysis [3], and detection in separation science including chromatography [4], capillary electrophoresis [5–7], as well as non-chip [7] and on chip microfluidic platforms [8]. Radiometric characterization of LEDs provides valuable information directly related to the sensitivity (such as in fluorimetric detection) and other performance parameters of optical detection systems (such as baseline noise in absorption photometric detection) [9].

The use of LEDs extends far beyond analytical chemistry, both in science and industry, in areas including photochemistry, photopolymerisation, photosynthesis, sterilization, security, medical imaging and many others. For example, LEDs as quasi-monochromatic light sources with emission bandwidths as full width at half maxima (FWHM) typically 10–50 nm, are often the preferred light source for photo polymerization over the conventional broadband light sources [10,11], where radiometric power output (also termed as radiant flux, defined as emitted radiometric energy per unit of time, in Joule/sec or watt) plays a vital role in photo ionization. In most cases the incident power of the deployed LED is either measured using radiometers or depends on optical output data supplied by the manufacturer [12] However, Price et al. [12] reported that neither the measured radiometric power output from commercial radiometers nor the vendor provided data

* Corresponding author.
E-mail address: mirek.macka@utas.edu.au (M. Macka).

https://doi.org/10.1016/j.snb.2018.01.179
0925-4005/

were in agreement with the acquired radiometric output of the LEDs in the light curing unit (LCU) for photo polymerization. In other applications such as, photo sterilization, high irradiance (i.e., emitted radiometric power impinged onto an area, W/m^2) is the most important parameter in order to effectively destroy the DNA of microbes [13]. UV LEDs are widely used for water sterilization [14] as well as for photocatalytic oxidation [15], where radiometric characterization of LEDs in terms of radiometric power is a prerequisite, as it directly affects the rate of the reaction [16] Likewise for other photoreactions, for instance photosynthesis [17], radiometric power measurements are carried out frequently. Therefore, radiometric characterization of LEDs is necessary in numerous areas of both analytical (especially in optical methods and optical detection methods) and nonanalytical utilizations in science and industry. Further, radiometric power values of light sources are crucial for establishing their radiant efficiency (%) (also termed as external quantum efficiency, energy conversion efficiency or wall plug efficiency, defined as the % fraction of the input electrical power yielding light exiting the light source i.e., exiting optical power divided by the input electrical power).[1] The analytical use of LEDs from commercial vendors primarily for optical sensing and detection has increased over the past two decades exponentially [2] but there is a lack of simple and rapid method to characterise these LEDs as a prerequisite for any analytical use of LEDs.

Chemical Actinometry (CA) can be used to radiometrically characterize light sources, even though it has been reported only scarcely for LEDs for the measurement of their optical power output [13,18]. Photodiode measures the photocurrent resulting from incident light, which can be used to calculate the radiometric power output of the light source if the spectral responsivity (ampere/watt) of the photodiode is known. To the contrary, a fundamental strength of CA is that from its principle it is an absolute method, as it directly measures the number of mole of products reacted in a photochemical reaction at a given wavelength, which can then be used to calculate absorbed photon during the photochemical reaction using an established actionometric solution given the quantum yield of the photochemical reaction at that particular wavelength is known. The quantitation can be accomplished titrimetrically, although photometry is nowadays often used for convenience. While the loss of incident light may register a lower radiometric power output than the actual one by a photodiode, the known quantum yield of the photochemical reaction will always produce an accurate result of photon absorption and hence, chemical actinometry facilitates the most accurate method to measure the incident light. Although CA is the most accurate radiometric method [19], it is time consuming, needs skilled experimentation, and depends on purity and stability of standard actinometric chemicals. Nonetheless CA is a simple and essentially non-instrumental method that can be used to independently cross-validate other radiometric methods [20].

Spectrophotometers are used to measure the emission spectra of LEDs, but from the conventional normalized emission spectra of LEDs only information on bandwidths and emission wavelengths maxima can be obtained [21]. Quantitative information regarding crucial radiometric power cannot be extracted from the raw LED spectra (in relative intensity units) without a calibration. Any calibration is however associated with one specific optical design and geometry, such as a CCD spectrophotometer, the distance of the LED from the entrance slit etc. If the design changes, the calibration becomes invalid, and cannot be used for other optical designs and geometries. This limitation applies to measurements of radiometric power in many other important non-analytical applications such as germicidal applications, UV dosimetry, photopolymerisation and many others. Hence accurate and precise measurement of the radiometric power output of the LEDs from the emission spectra obtained from spectrophotometers is difficult.

For measuring radiometric power output, the International Commission On Illumination (Commission Internationale de l'Éclairage, CIE) have established a standard method using a spectrophotometer with an integrating sphere (IS) [22]. Although this method is well established, it requires specialized instrumentation including an IS and a calibrated light source, which must be regularly recalibrated. Furthermore, there are reports that this method can suffer from significant systematic errors. Optical Technology Division of National Institute of Standards and Technology (NIST) reported significant fluorescence from the IS coating material while measuring radiometric power output of UV [23,24] and deep blue LEDs [24]. As an alternative to IS, researchers also employed a cosine corrector (CC) (used with a spectrophotometer) [17], which are optical diffusers made of opaline glass, polytetrafluoroethylene (PTFE) or Spectralon® for radiometric characterization of LEDs. A principal problem is that coating materials of both IS and CC (i.e., either Spectralon® or PTFE) are extremely prone to contamination in unclean environmental conditions [25] and may also get contaminated during the manufacturing phase [26]. Contaminated IS or CC are known to cause considerable errors and especially overestimation of the radiometric power outputs of LEDs [24,26]. The Optical Technology Division of NIST employed correction software to overcome the difficulties involving IS and CC during radiometric characterization of LEDs using a spectrophotometer [24], however, it makes the calculation complex and measurement process cumbersome. Moreover, measurements involving IS or CC with a spectrophotometer relies on an expensive calibration light source with limited design life (typically 50 h).

To the contrary, silicon photodiodes (Si-PD) have demonstrated accurate response for a wide range of light irradiations from 1 pW/cm^2 to 100 mW/cm^2 [27] and simple Si-PDs, without an integrated amplifier, are free from gain peaking problems [28]. In addition to those advantages, spectral response curves are known for Si-PDs (in most cases provided by the manufacturer) so that radiometric power can be calculated directly from measured photocurrent at a given wavelength. Therefore, the radiometric power of an LED could be potentially measured in a very straightforward rapid and low-cost manner for such optical designs and geometries where the LED light is collimated so that it can fall within the active area of a large area Si-PD, and for quasi-monochromatic LEDs (as opposed to white LED). Some manufactures offer information on using their Si-PD for radiometric characterization of LEDs [28], however, without any specifications of geometric and optical design of the method. For example, [28] only provides a brief note of the possibility of obtaining radiometric data through Si-PD in principle without enough details on the conduct of the measurements and the supporting evidence that the measurements provide reliable data, based on studying the distance, directivity, and uncertainty, as we offer here in our work. However, most importantly, no studies are available that would provide assurance of accuracy of radiometric values for such approach based on cross-validation of this approach with other independent methods.

Hence, in this study, we aimed at achieving the following goals: (i) Develop a technique using a simple large area silicon photodiode in a straightforward optical design that can provide for accurate, facile, robust, and low-cost radiometric characterization of LEDs in terms of irradiance and radiometric power output. We demonstrate this for 21 commercial LEDs through a wide range of wavelengths from deep UV to NIR (255–950 nm), showing that this technique is applicable to various sensing and analytical systems in a rapid, facile and inexpensive manner. (ii) We cross-validate the

[1] In this work, we use radiometric units, in difference to photometric units used in areas defined for the purpose of human vision such as lighting (candelas or lumens), see Fig. S2 A&B and Table S2.

method by comparison with 2 independent methods and established radiometric methods, namely chemical actinometry, and spectral radiometry using a calibrated spectrophotometer. (iii) Further we demonstrate the practical implications of the method by accurately determining quantum yields and fluence values of conventional actinometric systems in rapid and facile manner. (iv) Finally, we discuss further implications in other areas such as radiometric characterization of polychromatic light sources of any shape where no standard actinometric methods are available.

2. Instruments and methods

2.1. Chemicals and reagents

Potassium iodide (KI), borax ($Na_2B_4O_7$), potassium ferrioxalate $K_3[Fe(C_2O_4)_3]\cdot 3H_2O$, Reinecke's salt as ammonium Reineckate $NH_4[Cr(NCS)_4(NH_3)_2]\cdot 0.66H_2O$ and 1,10-phenanthroline were obtained from Sigma Aldrich, Australia. Sodium oxalate ($CH_3COONa\cdot 3H_2O$), Potassium iodate (KIO_3) and potassium nitrate (KNO_3) were purchased from BDH Prolab Chemical, Australia. Perchloric acid (70%) ($HClO_4$) and sulfuric acid (H_2SO_4) (95–98%) were obtained from Univar, Australia. Ferric nitrate ($Fe(NO_3)_3$) was purchased from Chemical supply, Australia, Sodium oxalate ($C_2Na_2O_4$) from BDH (VWR) Chemicals, Australia. Deionized water (Millipore, Bedford, MA, USA) was used to prepare all solutions.

2.2. Instrumental

Instruments used in this experiment were commercially procured and listed in the ESI Section 1 with details. The details for LEDs and silicon photodiode are given below.

2.2.1. LEDs

Commercially available 21 LEDs in the range from UV to near infrared wavelengths (255–950 nm) were used in this work are listed with their vendor provided specifications in the electronic supporting information (ESI) Table S1. LEDs in the range 360–950 nm had integrated water clear hemispheric silicone and epoxy lenses (diameter 5 mm), while the two deep UV LEDs (λ_{max} = 255 and 280 nm) were equipped with metal can package TO-39 (which also acts as heat sink) and encapsulated UV transparent glass ball lenses.

2.2.2. Si-photodiode (Si-PD)

A UV enhanced Si-PD (Normal Response, 100 mm^2, Edmund optics, Woodlands Loop, Singapore) was used in this study to measure the radiometric output power of the LEDs. The outer diameter of this photodiode was 25 mm where the active (sensitive) area was 100 mm^2. The responsivity range of this photodiode was from 200 nm to 1100 nm.

2.3. Method

2.3.1. Emission spectra acquisition

To obtain LED emission spectra in absolute units (watt nm^{-1}), the observed detector response (R_{obs}) in count representing the emission spectra was corrected for applied forward current (I_F), maximum forward current (I_{max}), Integration time (IT) and the spectral response of the CCD (S_{CCD}) (described in ESI Section 4) resulting the absolute detector response (R_{abs}). The arrangement of this measurement is shown in Fig. S1a(i) and S1b(i).

To obtain conventional LED emission spectra in arbitrary units, however at comparable conditions, we also normalized all LED spectra against the maximum intensity (count) of the corresponding LED [2].

2.3.2. Radiometric power output measurement using silicon photodiode (Si-PD method)

The radiometric power output of each LED for the maximum allowable forward current I_{max} of respective LEDs was determined by measuring the photocurrent of the Si-PD with a digital multimeter. Detail of this method is described in ESI section 5 and both schematic and pictorial representation of the method is shown in Fig. S1a(ii) and S1b(ii), respectively.

2.3.3. Radiometric power output measurement using chemical actinometry

Three different standard chemical actinometers (I^-/IO_3^-, $K_3[Fe(C_2O_4)_3]\cdot 3H_2O$, and $KCr(NH_3)_2(NCS)_4$) were deployed to determine the radiometric power output of eight different LEDs with maximum wavelength of λ_{max} = 255, 280, 380, 420, 500, 545, 605, 750 nm from the same 21 LEDs as described in ESI section 6 with actinometric standard solution preparations and the arrangement for the chemical actinometric measurement is illustrated in Fig. S1a(iii) and S1b(iii).

2.3.4. Irradiance measurement using Si-PD and spectrophotometer

We determined Irradiance values for the 21 LEDs using the radiometric power output values obtained with the Si-PD applying the inverse square law of electromagnetic radiation at 3 cm distance. According to the inverse square law of electromagnetic radiation, the irradiance of a light source is proportional to the inverse of the squared distance of measurement as shown in Eq. (3) [29].

$$E = \frac{I}{d^2} \tag{3}$$

where, E = irradiance of the light source in watt/cm^2, I = radiant intensity in watt per steradian and d = distance of measurement in cm. In order to calculate the irradiance at any other distance, Eq. (3) can be rewritten as:

$$E_1 {d_1}^2 = E_2 {d_2}^2 \tag{4}$$

We then calculated the irradiance E_2 by dividing the radiometric power output measured by Si-PD by the effective area of illumination at distance d_2 (Figs. S1a (ii) and S6 in ESI). The irradiance E_1 at distance d_1 (in this study we used d_1 = 3 cm as we optimised this distance for emission spectra acquisition) could then be easily calculated using Eq. (4). We utilised the full viewing angle of the LEDs provided by the vendor for effective area calculation. The details of effective illuminated area and distance calculations are provided in ESI Section 7.

In order to verify the accuracy of the calculated values of irradiances E_1 (at distance 3 cm) by facile Si-PD method, we calculated irradiances from the emission spectra of LEDs. Irradiances from the emission spectra of LEDs (SP method) were obtained by dividing the integrated area of each spectrum in absolute units (spectral radiant power) shown in Fig. 1B with the effective illuminated area at 3 cm distance. Here the effective illuminated area was the area of the entrance slit of the spectrophotometer and was calculated by considering the entrance slit of the spectrophotometer as a circle of 25 μm diameter according to the specification. So this means that here in our study we demonstrated that irradiance can be accurately calculated at any distance from the LED using our Si-PD method by simply employing the inverse square law of electromagnetic radiation.

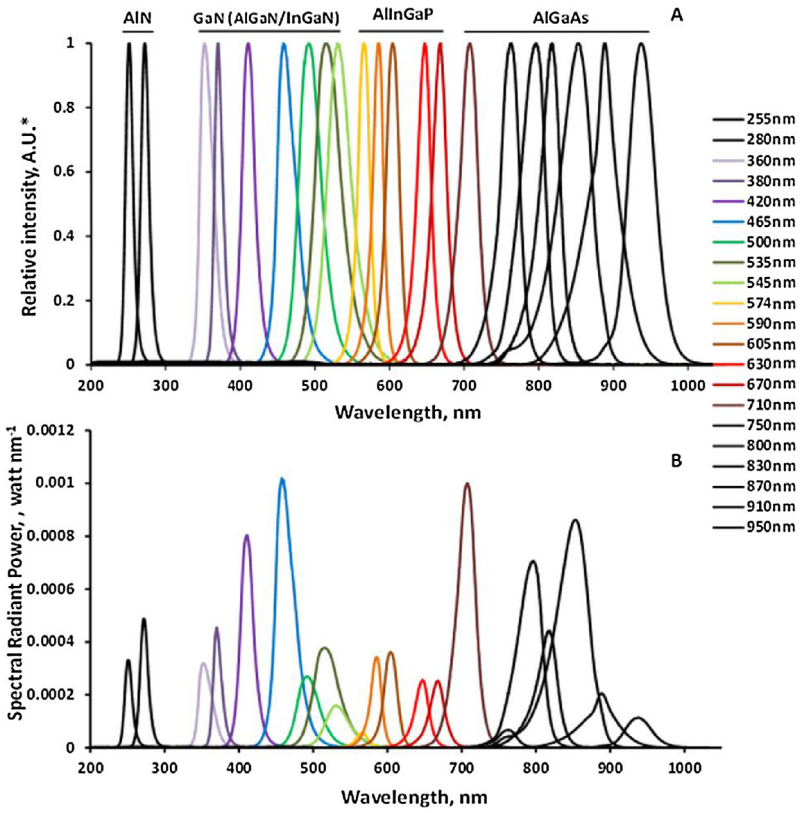

Fig. 1. Emission spectra of 21 LEDs (A) normalized against maximum spectral response (in *arbitrary unit A.U.) (B) corrected emission spectra (as spectral radiant power) of the 21 LEDs expressed in absolute units (watt/nm). Conditions of the experiment: SP (USB2000 + XR1-ES), axial distance between the SP and LEDs = 30 mm, spectral responses corrected for forward current, integration time and spectral sensitivity of CCD of the SP, information regarding semiconductor materials of the LEDs were supplied by the vendors.

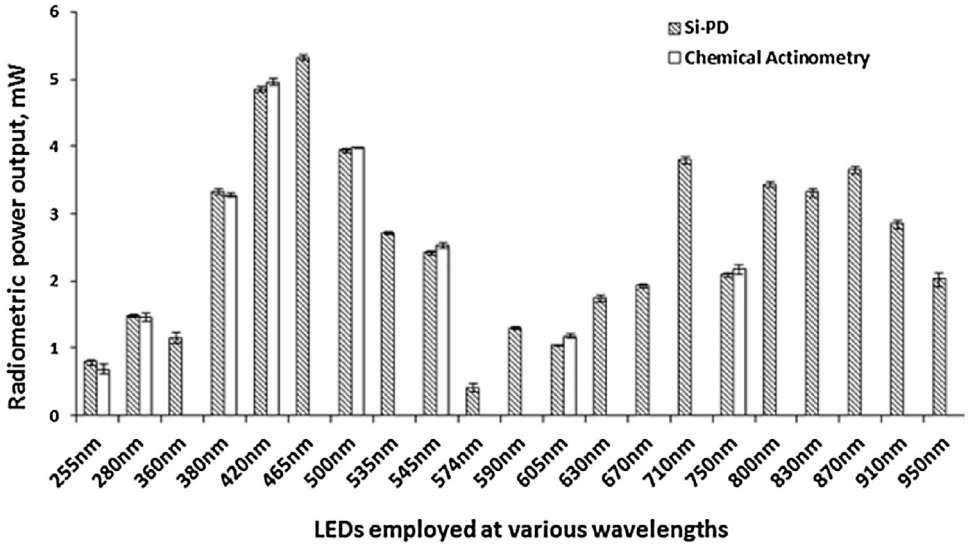

Fig. 2. Comparison of the radiometric power output of LEDs (UV–vis-NIR) using Si-PD and chemical actinometry method, conditions: Si-PD and cuvette containing actinometric solution were adjacent with LEDs as shown in Fig. S1 B and C. Error bars represent standard deviation from the average of five replicate measurements.

3. Results and discussions

3.1. Emission spectra

Emission spectra are one of the most important characteristics of an LED. Traditionally emission spectra are measured with a spectrophotometer, with the relative intensity given in arbitrary units when the geometry and the resulting % of emitted light detected is not known. This is shown in Fig. 1A featuring emission spectra of 21 commercial LEDs in spectral range from deep UV to NIR. Such normalized graphs allow a clear comparison of emission maxima and bandwidth values for different LEDs (see Table S1), reflecting the semiconductor type and properties [30] (semiconductor type typical in a particular wavelength area given in Fig. 1A).

The emission spectra in Fig. 1A in relative intensities given in arbitrary units, however, do not allow any quantitative comparison

of emission intensities for the LEDs as they do not give any quantitative information about the LED radiometric power (W) or irradiance (W/m^2). In this section, we demonstrate a simple way to convert the initially measured intensities in counts into absolute units as shown in Fig. 1B. The spectral radiant power, which is effectively the spectral distribution of radiometric power output over the wavelength range, is shown in Fig. 1B (W/nm). It was obtained from the spectrophotometer relative intensities (in counts) converted to spectral radiant power (W/nm) using a CCD responsivity curve (shown in Fig. S5), which is effectively an array of calibration factors (as many calibration factor numbers as many wavelength, count.nm/W). This responsivity curve is obtained by measuring response for a calibrated light source (shown in Fig. S4). Importantly, it is valid only for a specific geometry and optical configuration (if any element between the light source and the CCD spectrophotometer changes, the calibration is invalid and a new one has to be recorded). For each LED, the area under the emission curve gives the radiometric power output (W) entering the spectrophotometer for a given geometry and optics (including the LED integrated lens). Due to the in principle undefined spectrophotometer geometry, the % fraction of the light detected is unknown, but equal for all LEDs, and therefore it allows quantitative comparison of their optical power output across a range of wavelengths.

From the spectral radiant power graph (Fig. 1B) several observations can be made: (i) quantitatively comparable intensities of different LEDs can be very different; (ii) they tend to vary with emission maximum wavelength, with the blue LEDs and far red to NIR LEDs offering the highest intensities (spectral radiant power). This observation correlates with the general notion about different LED intensities at different wavelength ranges. Both observations are the result of different semiconductor materials used in different LEDs, producing different radiant efficiency values, and additionally of higher steady (constant) current for NIR and UV LEDs [30,31].

When it comes to the aforementioned irradiance, the fraction of the detected light does not represent the total radiometric power output of the LED, therefore the integrated area from the resulting fraction of detectable light cannot be directly considered as total radiometric power output. However, irradiance (defined as radiometric power output in a unit of area, also refer to the scheme in Fig. S6) can be calculated from the integrated area of the quantified spectral radiant power emission spectra (Fig. 1B) by defining the effective illuminated area, for LEDs with integrated collimating lens and therefore relatively narrow viewing angle values (<30°) (see Fig. S6 in ESI), which is given by the manufacturer. In the next section, we will show that we can measure total radiometric power output of LEDs using Si-PD, partial radiometric power output from emission spectra of LEDs and irradiance values calculated from the partial radiometric power output determined from the emission spectra. Furthermore, we will show in the following section that such irradiance values can be used to correlate quantitatively with irradiance values obtained through the Si-PD-based radiometric method.

3.2. Radiometric power output

Radiometric power is the principal indicator of total optical output of a light source considered when using LEDs in analytical chemistry to consider in their optical detection and other applications (for instance unlike in lighting for humans, see scheme of radiometric and photometric units in the ESI Fig. S3B).

For accurate evaluation of radiometric power output of LED, the entire emitted radiation (radiation capture close to 100%) needs to be measured. As mentioned earlier, most of the existing methods for radiometric power output may be unreliable, convoluted and expensive, we used a simple Si-PD with relatively large photosensitive area (100 mm^2) which captures close to 100% of the light emitted by the LED falling within the active sensitive area of the Si-PD.

To investigate the radiation captured for the 21 LEDs used in this study, first we considered the likely radiation capture (%) based on the geometry and the vendor provided directivity plots of each LED in Fig. S7). The directivity plot of LEDs is an established method developed by Commission Internationale de l'Éclairage (CIE) [22] to indicate the spatial distribution of the emitted radiation (in terms of radiant or luminous intensity) from the LEDs.

By definition, 50% of the maximum emitted radiation from the LED can be measured/observed if the detector is positioned at the vendor specified full viewing angle ($2\theta_{1/2}$) which is a function of LED chip type and the lens that distributes the light [32]. From the directivity plots of 21 LEDs in this study, we observe that the maximum angles of spread of radiation emitted from the LEDs are 3–5 times larger than the reported viewing angles (see Fig. S7). In this study, instead of measuring radiant or luminous intensity by radiometric procedures that are well established but may be regarded as expensive and cumbersome, we utilized the radiometric power output of LEDs measured at different distances from the LEDs by the Si-PD method as an indicator of radiation capture % shown in Figs. S8A and S8B . We observed the radiometric power output by placing the LEDs at different distances from the silicon photodiode and found that the radiometric power output starts attenuating at distance over ca. 10 mm for LEDs with wider full viewing angle $2\theta_{1/2} = 20°$ and 30°, whereas no attenuation was observed up to 10 mm distance for LEDs with narrow viewing $2\theta_{1/2} = 16°$. At 2.34 mm distance from the LED, (the minimum distance with the LED touching the Si-PD) the total photosensitive area (100 mm^2) of the silicon photodiode used in this study subtended a solid angle $\Omega = 18.36$ sr at the goniometric centroid of the LEDs. Goniometric centroid is the precise position of the emission centre of the LED [33] and according to CIE 2007 [22] the front tip of the LEDs with hemispheric lenses is the emission centre. Therefore, the calculated solid angle (18.36 sr) is 11 times larger than the solid angle subtended at the goniometric centroid of an LED due to the largest reported spread of radiation (85° as reported in Fig. S7 LED directivity plot in ESI) in this study. Hence, we emphasize that by ensuring a large enough solid angle at the goniometric centroid of the investigated 21 LEDs in this study, we have to a satisfactory degree eliminated the loss of radiation emitted from the LEDs. However, we acknowledge the fact that LEDs with other types of lenses than those reported in Table S1 (Vendor specified LED specifications given in ESI), for polychromatic radiation and for viewing angles larger than in this study will exhibit different directivity of radiation, and hence will require careful observations of their directivity plots while reporting their radiometric power outputs.

In Fig. 2, the measured radiometric power outputs of the LEDs are shown. The obtained results from the Si-PD method was compared with chemical actinometry and the two methods established good agreements where coefficient of variations (COV) ranged from 0.6% to 15% (Si-PD method) and 0.3% to 10% (actinometric method). Although there were no established chemical actinometers at longer wavelength than 795 nm, the excellent agreements amongst the two methods in the UV–vis wavelengths range available for actinometric measurements allowed us to conclude that similar relationships can be expected at higher wavelengths outside the actinometry spectral range (750–910 nm).

3.3. Irradiance

In optical measurements, the geometry of the optical de-sign plays a significant role. To acquire emission spectra of a wide range of LEDs (as described in experimental section) we used a specific geometric setup (Fig. S1a(i)) which was different from the geomet-

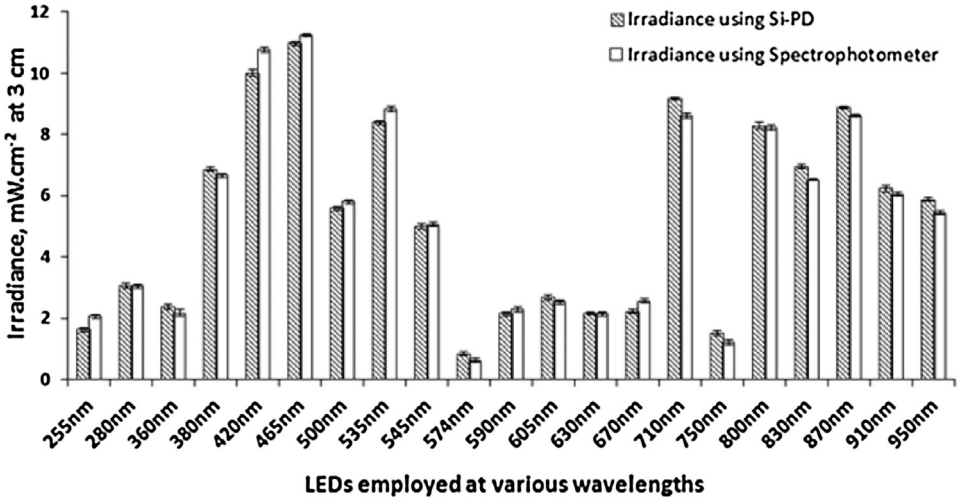

Fig. 3. Comparison of irradiance values determined at 3 cm distance using Si-PD method and measured from emission spectra using spectrophotometer. Error bars represent standard deviation from the average of five replicate measurements.

ric setup used in the Si-PD and actinometric methods as shown in Fig. S1a(ii) and S1a(iii), respectively. Whilst the silicon photodiode used in Si-PD method (Fig. S1a(ii)) and the cuvette used in actinometric method (Fig. S1a(iii)) were placed directly in front of the LEDs, the spectrophotometer used in the emission spectra acquisition (Fig. S1a(i)) had to be placed at 3 cm from the LEDs in order to avoid the CCD counts being out of range resulting from incident light emitted from the wide ranges of UV–vis-NIR LEDs used in this study. Therefore, based on this rationale, it can be expected that the radiometric power outputs measured from the emission spectra would vary from either measurement by Si-PD or actinometric methods. However, by definition, the irradiance (i.e., power measured per unit area) of any light source measured at a particular distance would be the same. Hence, we compared the irradiances at 3 cm from the LEDs measured from the absolute emission spectra with that measured from the Si-PD method as shown in Fig. 3. The coefficients of variation ranged from 0.5% to 7% in SP method and from 0.3% to 10% in Si-PD method for UV to NIR LEDs. Hence, these excellent agreements between the irradiances measured by Si-PD method and that from the emission spectra reconfirmed the accuracy of the radiometric Si-PD method for a very wide range of wavelengths from 255 nm to 950 nm.

3.4. Radiant efficiency (η_r)

Almost in all cases, the efficiency of LEDs is considered as electrical to optical power conversion ability (i.e. wall-plug efficiency) to describe its light output capability [34,35]. However, in many analytical as well as industrial applications, it is equally important to know the radiometric power conversion efficiency (Eq. (5)) to quantify the radiant power output ability of LEDs in a rapid manner. This efficiency not only shows an excellent balance between quality control and cost-effectiveness of the radiant source but also indicates the capability of an LED for its ultimate utilization of radiometric power. Calculated η_r of all the 21 LEDs are shown in Fig. 4.

Fig. 4 shows that the blue LEDs (λ_{max} = 465 nm) are the most efficient in terms of radiant efficiency (ca. 17%), whereas the η_r of deep UV LEDs are the lowest amongst all other LEDs (0.1–0.2%). These differences are caused by different properties of different semiconductors. Efficiency of LED devices depends on photon emission which is the consequence of electron-hole recombination in the semiconductor materials. The electron-hole recombination is much slower for aluminium nitride (AlN) based semiconductors [31,36] that constitute the deep UV LEDs. Hence, in our study the determined values of η_r for the deep UV LEDs were very low. Low η_r values for the deep UV LEDs can be also attributed to the 'efficiency droop' phenomenon of LEDs. According to the US department of Energy, the efficiency of an LED decreases when operating it with higher electric current [37]. In our study, the applied current for the deep UV LEDs were 5 times higher than the visible LEDs, which may contribute to the efficiency droop. For the visible LEDs the η_r ranged from 1% (yellow at λ_{max} = 575 nm) to 17% (royal blue at λ_{max} = 465 nm), which agrees well with the efficiency values reported by Kraft makher [38]. Although the other two UV LEDs (λ_{max} = 360 nm, 380 nm) were based on the same semiconductor material gallium nitride (GaN) as blue and green LEDs, their emission at shorter wavelength could cause thermal rise within the package, which consequently downgraded the efficiency of these UV LEDs [31].

Red LEDs (λ_{max} = 605, 630, 670 nm) revealed efficiencies ranging from 2% to 6% whereas, efficiencies slightly increase in the NIR region ranging from 4%-10%. These differences come from differences in semiconductor materials. Aluminium gallium arsenide (AlGaAs), which are the semiconductor materials in NIR LEDs (λ_{max} = 710, 750, 800, 870, 910, 950 nm), were reported having higher efficiency than aluminium indium gallium phosphide (AlInGaP) which are the semiconductor materials in red LEDs (λ_{max} = 605, 630, 670 nm) [39].

3.5. Uncertainty

The NIST has stipulated that the expanded uncertainty (coverage factor K = 2 for 95% level of confidence) of any radiometric measurement needs to be reported for quality assurance and quality control purposes [40]. Table 1 illustrates the uncertainties associated with various radiometric parameters measured in this study. We found that the radiometric parameters measured in this study (particularly by the Si-PD method) were associated with lower uncertainties compared to other studies as shown in Table 1.

3.6. Implications to quantum yield (QY) measurements

We utilized the radiometric power outputs measured by the Si-PD method to calculate the QY of different actinometric systems at different wavelengths and the results are shown in Table 2. The excellent agreements between the calculated QY and the reported QY from literatures shows that the facile Si-PD method can be employed for rapid and accurate determination of QY of in princi-

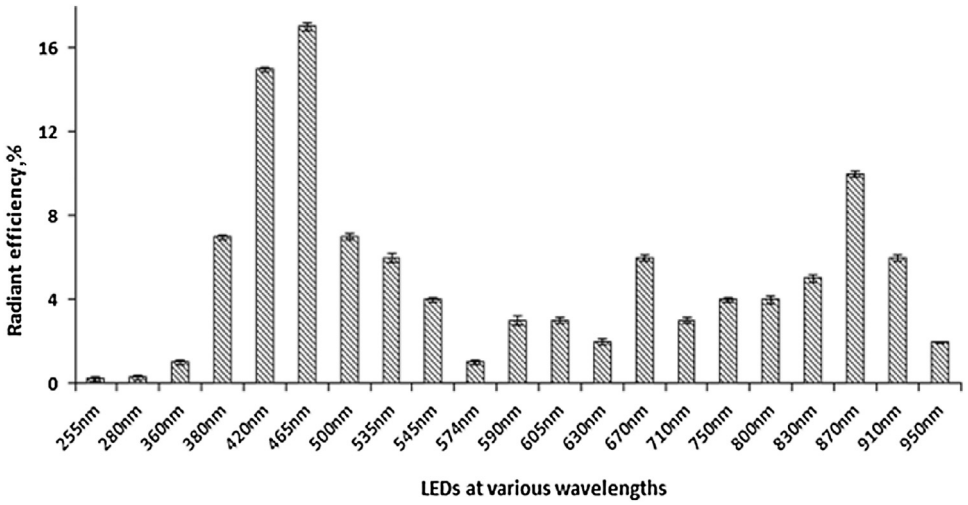

Fig. 4. Radiant efficiency (η_r) of UV–vis-NIR LEDs. Error bars represent standard deviation from the average of five replicate measurements.

Table 1
Uncertainty values associated with radiometric parameters of LEDs using various methods and in this study*.

Radiometric Parameters Measured	Method Employed	Uncertainties reported
Radiometric power output	Si-PD method	0.3–5%*
	Source-based method	5.8% [24]
Irradiance	Detector-based method	5.2% [24]
	Si-PD-method	0.2–7%*
Radiant efficiency	SP-method	0.5–6%*
	Si-PD method	0.7–6%*

Table 2
Comparison of QY values calculated from Si-PD method with existing literature values of three standard chemical actinometers at different wavelengths.

Actinometer	Wavelength	QY	
		Si-PD method	Literature Value
KI-KIO_3 actinometer	255 nm	0.707 ± 0.051	0.73 ± 0.02 [44]
	280 nm	0.287 ± 0.06	0.3 [44]
$K_3[Fe(C_2O_4)_3]\cdot_3H_2O$	380 nm	1.007 ± 0.015	1.13 [45]
	420 nm	0.9 ± 0.07	1.12 [45]
	500 nm	0.81 ± 0.05	0.86 [46]
	545 nm	0.147 ± 0.023	0.15 [46]
Reinecke's salt actinometer	600 nm	0.276 ± 0.0316	0.28 [45]
	750 nm	0.22 ± 0.062	0.27 [21]

ple any photochemical reaction. The advantage of the Si-PD method can be realized particularly during the determination of the number of moles of photons produced in a photochemical reaction, where the current practice requires laborious, time-consuming and expert chemical actinometric studies. The detailed calculations of QY with Si-PD method are illustrated in ESI Section 6.4.

The value of this approach further extends to poly-chromatic light sources. Einschlag et al. [41] utilized QY values at different wavelengths in a ferrioxalate actinometer to measure the incident photon rate from polychromatic light source such as a medium pressure tubular mercury lamp. However, the QY values may not always be readily available at a desired wavelength within the emission spectrum of a polychromatic light source. In this context, the calculated QY values for a suitable photochemical reaction at the desired wavelength by the Si-PD method of this study have the potential to radiometrically characterize polychromatic light sources of any shape where no standard actinometer is available.

3.7. Implications to fluence measurement

Fluence refers to incident radiant energy in a small space from all angles. Fluence measurement is particularly important where total radiant energy from a light source impinges on a targeted small region, for instance, UV water disinfection or any other germicidal radiation. It is usually calculated by studying photoreactions in actinometric systems [42,43] following Eq. (S14) in ESI.

Table 3
Comparison of fluence values for Iodide-iodate actinometric system obtained by using Si-PD method and compared with reported literature values .

Wavelength	Fluence, mJ cm^{-2}	
	Si-PD method	Literature value
255 nm	80.06 ± 0.8	82 ± 0.07 [43]
280 nm	36.7 ± 0.21	37.94 [13]

We utilized the proposed Si-PD method to calculate the QY of the germicidal reaction as mentioned by Rahn et al. [44] and used Eq. (S14) to calculate the fluence. The results were in good agreements (80–97%) as shown in Table 3.

4. Conclusions

The work presented here has extensive implications to broad areas of analytical chemistry where light sources are used that

need to be properly characterised. We established that the method using a silicon photodiode by assigning straightforward geometry and calculations allows a facile, rapid, inexpensive and accurate determination of radiometric power output and irradiance of LEDs across a wide spectral emission range from UV to NIR. Chemical actinometric methods can be used to measure radiometric power independently and also to validate the accuracy of the silicon photodiode radiometric power measurements. Spectrophotometric measurement of irradiance values of the LEDs ranging from deep UV to near infrared wavelengths further validated the radiometric data. The COV within 5% (when compared radiometric power outputs with actinometric methods) and 2% (when compared irradiances with spectrophotometric methods) revealed the accuracy of the silicon photodiode method. Additionally, implications of this method in terms of quantum yield and fluence measurement in a facile, rapid, accurate and inexpensive manner were illustrated and excellent agreements with existing studies were reported. Therefore, the use of this method for radiometric characterization of the LEDs can be further extended to areas such as photo sterilization and photoreactions (e.g., photo polymerization, photosynthesis and photocatalytic reaction) as well as for characterizing non-point light sources and poly-chromic light sources.

Acknowledgments

MM acknowledges his ARC Future Fellowship Level 3 (FT120100559). MD acknowledges Materials Research Centre at FCH BUT-Sustainability and Development, REG LO1211, with financial support from National Programme for Sustainability I (Ministry of Education, Youth and Sports), and also Financial support from the Academy of Sciences of the Czech Republic (Institute Research Funding RVO:68081715) is gratefully acknowledged. The authors would also like to acknowledge John Davis from the Central Science Laboratory for assistance with electronics. The authors have declared no conflict of interest.

Appendix A. Supplementary data

Supplementary data associated with this article can be found, in the online version, at https://doi.org/10.1016/j.snb.2018.01.179.

References

[1] D.A. Bui, P.C. Hauser, Analytical devices based on light-emitting diodes—a review of the state-of-the-art, Anal. Chim. Acta 853 (2015) 46–58.
[2] M. Macka, T. Piasecki, P.K. Dasgupta, Light-emitting diodes for analytical chemistry, Annu. Rev. Anal. Chem. (Palo Alto Calif.) 7 (2014) 183–207.
[3] S.D. Smith, A. Vass, F. Karpushko, H. Hardaway, J.G. Crowder, The prospects of LEDs, diode detectors and negative luminescence in infrared sensing of gases and spectroscopy, Philos. Trans. R. Soc. A: Math. Phys. Eng. Sci. 359 (2001) 621–634.
[4] B. Bomastyk, I. Petrovic, P.C. Hauser, Absorbance detector for high-performance liquid chromatography based on light-emitting diodes for the deep-ultraviolet range, J. Chromatogr. A 1218 (2011) 3750–3756.
[5] S. Sharma, L.T. Tolley, H.D. Tolley, A. Plistil, S.D. Stearns, M.L. Lee, Hand-portable liquid chromatographic instrumentation, J. Chromatogr. A 1421 (2015) 38–47.
[6] D. Xiao, L. Yan, H. Yuan, S. Zhao, X. Yang, M.M. Choi, CE with LED-based detection: an update, Electrophoresis 30 (2009) 189–202.
[7] M. Ryvolová, M. Macka, D. Brabazon, J. Preisler, Portable capillary-based (non-chip) capillary electrophoresis, TrAC—Trends Anal. Chem. 29 (2010) 339–353.
[8] F.B. Myers, R.H. Henrikson, J. Bone, L.P. Lee, A handheld point-of-care genomic diagnostic system, PLoS One 8 (2013) 9.
[9] Y. Li, P.N. Nesterenko, B. Paull, R. Stanley, M. Macka, Performance of a new 235 nm UV-LED-based on-capillary photometric detector, Anal. Chem. 88 (24) (2016) 12116–12121.
[10] X. Dong, W. Shen, P. Hu, Z. Li, R. Liu, X. Liu, Efficient benzodioxole-based unimolecular photoinitiators: from synthesis to photopolymerization under UV-A and visible LED light irradiation, J. Appl. Polym. Sci. 133 (2016) 43239–43249.
[11] C. Dietlin, S. Schweizer, P. Xiao, J. Zhang, F. Morlet-Savary, B. Graff, J.-P. Fouassier, J. Lalevee, Photopolymerization upon LEDs: new photoinitiating systems and strategies, Polym. Chem. 6 (2015) 3895–3912.
[12] R.B. Price, J.L. Ferracane, A.C. Shortall, Light-curing units a review of what we need to know, J. Dent. Res. 94 (2015) 1179–1186.
[13] C. Zeng, Application of UV LEDs for Turbid Wastewater Disinfection, Environmental Engineering and Management, School of Environment, Resources and Development, Asian Institute of Technology, Thailand, 2014, pp. 68.
[14] M. Mori, A. Hamamoto, A. Takahashi, M. Nakano, N. Wakikawa, S. Tachibana, T. Ikehara, Y. Nakaya, M. Akutagawa, Y. Kinouchi, Development of a new water sterilization device with a 365 nm UV-LED, Med. Biol. Eng. Comput. 45 (2007) 1237–1241.
[15] J. Kuipers, H. Bruning, D. Yntema, H. Rijnaarts, Wirelessly powered ultraviolet light emitting diodes for photocatalytic oxidation, J. Photochem. Photobiol. A: Chem. 299 (2015) 25–30.
[16] L.C. Ferreira, M.S. Lucas, J.R. Fernandes, P.B. Tavares, Photocatalytic oxidation of reactive black 5 with UV-A LEDs, J. Environ. Chem. Eng. 4 (2016) 109–114.
[17] R.Y. Jou, P.H. Lee, Measurement of light intensity profiles of light-emitting diodes in a cylindrical tank, Energy Procedia (2014) 1261–1265.
[18] R.M. Jenny, O.D. Simmons, M. Shatalov, J.J. Ducoste, Modeling a continuous flow ultraviolet light emitting diode reactor using computational fluid dynamics, Chem. Eng. Sci. 116 (2014) 524–535.
[19] J.N. Demas, R.P. McBride, E.W. Harris, Laser intensity measurements by chemical actinometry. a photooxygenation actinometer, J. Phys. Chem. (1976) 2248–2253.
[20] H.J. Kuhn, S.E. Braslavsky, R. Schmidt, Chemical actinometry, Pure Appl. Chem. 76 (2004) 2105–2146.
[21] L.T. Guide, The Radiometry of Light Emitting Diodes, 2018, https://www.labsphere.com/site/assets/files/2570/the-radiometry-of-light-emitting-diodes-leds.pdf (20 June, 2016).
[22] Measurement of LEDs, in: C.C.B. Commission Internationale de l'Éclairage (Ed.), International Commission on Illumination Provided by IHS Under License with CIE, 2007, Kegelgasse 27, A-1030 Vienna, Austria, pp. 40.
[23] C.C. Miller, Y. Ohno, Luminous flux calibration of LEDs at NIST, in: 2nd CIE Expert Symposium on LED Measurement, Gaithersburg, Maryland, USA, 2001, pp. 45–48.
[24] Y. Zong, C.C. Miller, K.R. Lykke, Y. Ohno, Measurement of total radiant flux of UV LEDs, in: CIE Expert Symposium on LED Light Sources, June 2004, Optical Technology Division, National Institute of Standards and Technology Gaithersburg, MD 20899, USA, Tokyo, Japan, 2004.
[25] P.-S. Shaw, Z. Li, U. Arp, H.W. Yoon, R.D. Saunders, K.R. Lykke, Characterization of Integrating Spheres for Ultraviolet Radiometry, National Institute of Standards and Technology, Gaithersburg, MD, USA, 2018.
[26] P.-S. Shaw, Z. Li, U. Arp, K.R. Lykke, Ultraviolet characterization of integrating spheres, Appl. Opt. 46 (2007) 5119–5128.
[27] D. Dobberpuhl, D. Johnson, Pulsed electrochemical detection at the ring of a ring-disk electrode applied to a study of amine adsorption at gold electrodes, Anal. Chem. 67 (1995) 1254–1258.
[28] Hamamatsu, Handbook of Si-Photodiode: Chapter 2, https://www.hamamatsu.com/resources/pdf/ssd/e02_handbook_si_photodiode.pdf (27 June, 2016).
[29] A.D. Ryder, The Light Measurement Handbook, Technical Publications Dept., International Light Technologies, 10 Technology Drive, Peabody, MA 01960, United State of America, 1997.
[30] X. Chen, A. Man Ching Ng, F. Fang, Y. Hang Ng, A.B. Djurišić, H. Lam Tam, K. Wai Cheah, S. Gwo, W. Kin Chan, P. Wai Keung Fong, H. Fei Lui, C. Surya, ZnO nanorod/GaN light-emitting diodes: the origin of yellow and violet emission bands under reverse and forward bias, J. Appl. Phys. 110 (2011) 094513.
[31] S. Nakamura, Current status of gaN-based solid-State lighting, MRS Bull. 34 (2009) 101–107.
[32] B.V. Heek, F. Rotberg, OVAB Europe white paper of viewing angle measurement, in: O.-o.-h.V.A. Bureauu (Ed.), Invidis Consulting GmbH for OVAB Europe, OVAB, Europe, Barco N.V. & invidis consulting GmbH, 81671 Munich/Germany, 2014, pp. 8.
[33] T. Nägele, R. Distl, Handbook of LED Metrology, Instrument Systems GmbH, version, Munich, (1999).
[34] S. Palakurthy, S. Singh, S. Pal, C. Dhanavantri, Design and comparative study of lateral and vertical LEDs with graphene as current spreading layer, Superlattices Microstruct. 86 (2015) 86–94.
[35] A.T.M.G. Sarwar, B.J. May, J.I. Deitz, T.J. Grassman, D.W. McComb, R.C. Myers, Tunnel junction enhanced nanowire ultraviolet light emitting diodes, Appl. Phys. Lett. 107 (2015) 101103.
[36] N. Shuji, S. Masayuki, I. Naruhito, N. Shin-ichi, High-brightness InGaN blue, green and yellow light-emitting diodes with quantum well structures, Jpn. J. Appl. Phys. 34 (1995) L797.
[37] U.S.D.O. Energy (Ed.), Energy Efficiency of LEDs, Office of Energy Efficiency & Renewable Energy, Washington, DC 20585, 2013.
[38] Y. Kraftmakher, Experiments with light-emitting diodes, Am. J. Phys 79 (2011) 825.
[39] D. Johnson, Pulsed electrochemical detection In liquid-chromatography, abstracts of papers of the american chemical society, in: Amer Chemical Soc 1155 16th St, Nw, Washington, DC 20036, 1994, pp. 71-ANYL.
[40] B.N. Taylor, C.E. Kuyatt, Guidelines for Evaluating and Expressing the Uncertainty of NIST Measurement Results, United States Department of

Commerce Technology Administration, National Institute of Standards and Technology (NIST), 1994, Technical Note 1297, 1994 Edition, pp. 24.
[41] F.S. Garcia Einschlag, L. Carlos, A.L. Capparelli, A.M. Braun, E. Oliveros, Degradation of nitroaromatic compounds by the UV-H2O2 process using polychromatic radiation sources, Photochem. Photobiol. Sci. 1 (2002) 520–525.
[42] R.O. Rahn, J. Bolton, M.I. Stefan, The iodide/iodate actinometer in UV disinfection: determination of the fluence rate distribution in UV reactors, Photochem. Photobiol. 82 (2006) 611–615.
[43] R.O. Rahn, S. Echols, Iodide/iodate chemical actinometry using spherical vessels for radiation exposure as well as for monitoring absorbance changes, Photochem. Photobiol. 86 (2010) 990–993.
[44] R.O. Rahn, M.I. Stefany, J.R. Bolton, Evan Goren, P.-S. Shaw, K.R. Lykke, Quantum yield of the iodide–iodate chemical actinometer: dependence on wavelength and concentration, Photochem. Photobiol. 78 (2003) 146–152.
[45] E.E. Wegner, A.W. Adamson, Photochemistry of complex ions. III. Absolute quantum yields for the photolysis of some aqueous chromium(III) complexes. Chemical actinometry in the long wavelength visible region, J. Am. Chem. Soc. 88 (1966) 394–404.
[46] C.G. Hatchard, C.A. Parker, A new sensitive chemical actinometer. II. Potassium ferrioxalate as a standard chemical actinometer, Proc. R. Soc. Lond. A: Math. Phys. Eng. Sci. 235 (1956) 518–536.

Biographies

Ansara Noori is a graduate student at the School of Physical Sciences, University of Tasmania. Her research interests include optical gas sensing with LEDs, portable analytical devices and optical detection.

Parvez Mahbub completed his PhD in environmental engineering from Queensland University of Technology in 2011 and post doctoral training at Australian Centre for Research on Separation Science at University of Tasmania in 2014. He is currently a Research Fellow at Victoria University at Melbourne working on freshwater sources and quality for aquaculture. His research interests span across environmental remediation, water quality engineering, flow based analytical systems, radiometry, sensor development and spectroscopy.

Miloš Dvořák received his PhD from the Brno University of Technology, and is currently a postdoctoral fellow at the Institute of Analytical Chemistry, Academy of Sciences of the Czech Republic, Brno, conducting research in capillary separations.

Arko Lucieer is an Associate Professor in Remote Sensing at The University of Tasmania, Australia. He leads the TerraLuma unmanned aircraft systems (UAS) research group, focusing on quantitative remote sensing of vegetation with the use of sophisticated UAS sensors to better understand the structure, distribution, and functioning of vegetation, and to bridge the observational scale gap between field samples and satellite observations.

Mirek Macka is an Australian Research Council Future Fellow and Professor at the Australian Centre for Research on Separation Science (ACROSS), University of Tasmania. His research encompasses areas of separation and detection science with emphasis on miniaturisation, instrumental design, and portable analysis, and specific focus on solid state light sources for optical detection and sensing.